

Ground state energy of a hard-sphere Fermi fluid

George A. Baker, Jr. and L. P. Benofy*

Theoretical Division, Los Alamos National Laboratory, University of California, Los Alamos, New Mexico 87545

Mauricio Fortes and Manuel de Llano†

Instituto de Física, Universidad Nacional Autónoma de México, 01000 México, D.F.

(Received 27 March 1986)

A new method of computing the ground state energy of a Fermi fluid is developed and applied to the hard-sphere Fermi fluids of two and four components. We find the results to be highly accurate for low densities. In this paper we compute and report the perturbation series for the ground state energy for the soft, repulsive, square-well problem at a number of densities for a four-component Fermi system as well as the ladder approximation energies for a hard-sphere potential at the same densities.

I. INTRODUCTION AND SUMMARY

In a recent series of papers¹⁻¹² a constructive method for the computation of the ground-state energy of various quantum fluids has been developed. The underlying idea can perhaps be traced back to van der Waals. It is very simply put: Instead of taking an ideal gas of point particles as the basic system to which corrections are to be made, one should take a gas of repulsive cores as basic and add to it, as a correction, the attractive interactions. The rationale for this idea is suggested by computer simulations for both classical and quantum systems which show that the hard-sphere pair distribution functions are qualitatively similar to those of Lennard-Jones liquid. This idea has led to a very successful theory¹³ of classical fluids.

In the course of work on our constructive methods for the ground-state energy it has become clear that the first and most important step is to develop a good representation of the hard-sphere ground-state energy. With this key piece of information, coupled with other known results, the methods permit accurate and fairly straightforward computation of the energy in most cases tried. In this paper we introduce a new method which we call the L expansion and apply it to the calculation of the ground-state energy of the simplest of repulsive cores, the hard sphere.

In Sec. II we introduce the L expansion. It differs from the well-known K -matrix expansion¹⁴ in the following way. The K -matrix expansion is basically a rearrangement of the Rayleigh-Schrödinger perturbation series in which infinite sums of diagrams replace the interaction vertices, and the remaining class of diagrams to be computed and summed is correspondingly reduced. In the L expansion, instead, the K -matrix energy itself is expanded and so too is the complete ground state energy; both are expanded in terms of a strength parameter. The K -matrix (or ladder approximation) series is reverted and substituted back into the complete series. The K -matrix corresponding to a hard-sphere system is computed by the solution of the appropriate integral equation and used as

the point at which to evaluate the L expansion.

In Sec. III we briefly describe the standard methods for the solution of the K -matrix equation and tabulate our results for the hard-sphere potential for ν =two- and four-component Fermi fluids.

In order to compute the L expansion it is necessary to expand the complete energy at various fixed densities in powers of the strength parameter for the repulsive square-barrier problem. This we do in Sec. IV. We summarize¹⁵ existing data for $\nu=2$ through fourth order, and we report the results of our computations for $\nu=4$ through third order. These results were obtained by means of Monte Carlo evaluation of integrals. We also add an additional density through third order for the $\nu=2$ case. These results, together with $\nu=1$ results for the third-order ring diagram, suffice to compute the series for the complete energy in powers of the repulsive strength through third order for any value of ν .

In Sec. V we combine the results of the preceding sections to compute the L expansion. We judge that the low-density results are very accurate and, in their region of validity, should serve as a standard against which other methods should be compared. The results extend the region of reliable information beyond that we had from our low-density expansions reported previously.^{3,5,12} Nevertheless, a full solution of the ground-state energy problem for fermion fluids requires (as was available for boson fluids) information from other sources at still higher densities.

II. THE L EXPANSION

As pointed out by Baker,¹⁵ the summability of the potential perturbation series with purely repulsive two-body interactions for the ground-state energy of a many-fermion system is under good theoretical control, even though this series is almost surely divergent. For practical purposes, however, some rearrangement has been considered desirable. Brueckner¹⁴ had the idea of rearranging into a single term all of the ladder diagrams. This procedure is sufficient for repulsive forces and avoids the added complexity of the R matrix¹⁵⁻¹⁷ expansion re-

quired when attractive forces are also present. The diagrams are illustrated in Fig. 1 using the notation of Hugenholtz diagrams. The right-pointing arrows are holes in the Fermi sea and the left arrows are excitations. After grouping the ladder diagrams into a sum, Brueckner's next step was to replace each vertex in the remaining diagrams by such a sum, thus constituting the "K-matrix rearrangement." The advantage of this new series is that its first term is exact in the low-density limit. The practical difficulty with this procedure is that the K matrices required depend not only on the momentum transfer at the vertex, as do the potentials in ordinary perturbation theory, but also on the exchanged momentum transfer, the total momentum, and the excitation energy of the Fermi sea. These additional dependences add considerably to the length of the computation.

We propose an alternate way to sum the perturbation series. It has the same basic advantages as the K -matrix rearrangement but is computationally simpler. In this paper we are ultimately concerned with the hard-core fluid. For this case the value of the ladder approximation to the energy shift ΔE (here we mean the difference between the ground state energy and the noninteracting Fermi sea ground-state energy) is finite. It will, of course, be non-negative for a purely repulsive potential and will correspond to no binding. Binding necessarily implies a negative binding energy. Thus if we have a central pair potential,

$$V(r) = v\Phi(r)(\hbar^2/Mc^2), \quad (2.1)$$

where M is the fermion mass, \hbar is Planck's constant over 2π , and c is a length, then for the hard-core case

$$\Phi(r) = \begin{cases} 1, & 0 \leq r \leq c \\ 0, & c < r, \end{cases} \quad (2.2)$$

$$v \rightarrow \infty,$$

we may write the ground-state energy series as

$$\frac{\Delta E M c^2}{N \hbar^2} = k_1 v + k_2 v^2 + k_3 v^3 + k_4 v^4 + \dots, \quad (2.3)$$

where the k_i are functions of the density. We may also write the ladder approximation to the ground-state energy as

$$L = \frac{\Delta E_L M c^2}{N \hbar^2} = m_1 v + m_2 v^2 + m_3 v^3 + m_4 v^4 + \dots, \quad (2.4)$$

where the m_i are also explicit functions of density. It is a straightforward matter, as $m_1 \neq 0$, to revert the series (2.4)

$$\frac{-3(-v)^n v}{8\pi k_F^3} \int d\tau \frac{\left[\prod_{j=1}^{n-1} \phi(|\mathbf{k}_{j-1} - \mathbf{k}_j|) \right] [\phi(|\mathbf{k}_0 - \mathbf{k}_{n-1}|) - \phi(|\mathbf{k}_0 + \mathbf{k}_{n-1}|) / v]}{\prod_{j=1}^{n-1} (k_j^2 - k_0^2)}, \quad (3.1)$$

where the region of integration is that allowed by the Pauli exclusion principle. The excitation lines have been labeled $(\frac{1}{2}\mathbf{p} \pm \mathbf{k}_j)$ for $j=1, \dots, n-1$ and the two hole lines $(\frac{1}{2}\mathbf{p} \pm \mathbf{k}_0)$. The function ϕ is the Fourier transform of $\Phi(r)$. We denote by ν the number of spin and isospin states available to each fermion, namely $\nu = (2S+1)(2I+1)$, where S and I are the spin and isotopic spins, respectively. The identity



FIG. 1. The ladder diagrams for the ground-state energy represented by the solution of the K -matrix equation. The right-pointing arrows are holes in the Fermi sea and the left-pointing arrows are filled states above the Fermi sea.

to give

$$v = n_1 L + n_2 L^2 + n_3 L^3 + n_4 L^4 + \dots, \quad (2.5)$$

where the n_i are explicit functions of the m_i and so explicit functions of density. The direct substitution of (2.5) into (2.3) yields what we call the L expansion,

$$\frac{\Delta E M c^2}{N \hbar^2} = p_1 L + p_2 L^2 + p_3 L^3 + p_4 L^4 + \dots, \quad (2.6)$$

where the p_i are explicit functions of the density, and of course $\Phi(r)$, as are the k_i , m_i , and n_i as well.

To use the L expansion for our computation of the ground-state energy of the hard-sphere Fermi fluid, we first compute the corresponding value of L by the solution of the K -matrix equations as described in the next section. Then we sum the expansion (2.6) for that value of L and so deduce the energy. Since L is exact in the limit of zero density, the higher order coefficients in (2.6) vanish in this limit and we expect (2.6) to be particularly useful for dilute systems and to be a definite improvement over the simple ladder approximation.

We remark that the arguments of Baker¹⁵ (see Sec. III C of that reference) applied to the L expansion indicate that it is likely to be an asymptotic expansion, but that at least we can bound

$$|p_j| \leq M_1 (M_2)^j j!, \quad (2.7)$$

where M_1 and M_2 are positive constants independent of j . It is possible, however,¹⁸ that although still an asymptotic series, the rate of divergence may not be as fast as allowed by (2.7).

III. K-MATRIX COMPUTATIONS

The general n -vertex term in the ladder sum of the ground-state energy diagrams (Fig. 1) is given by¹⁵ (see Sec. IV A of that reference)

$$(\frac{1}{2}\mathbf{p} + \mathbf{k}_j)^2 + (\frac{1}{2}\mathbf{p} - \mathbf{k}_j)^2 - (\frac{1}{2}\mathbf{p} + \mathbf{k}_0)^2 - (\frac{1}{2}\mathbf{p} - \mathbf{k}_0)^2 = 2(k_j^2 - k_0^2) \tag{3.2}$$

has been used to reexpress the denominator in (3.1). The formal sum of the ladder terms can be given in terms of the K matrix which in turn is the solution of the integral equations

$$K(\mathbf{k}', \mathbf{k}''; p, k_0) = v\phi(|\mathbf{k}' - \mathbf{k}''|) - v \int_{|\mathbf{k}''' + (1/2)\mathbf{p}| > k_F; |\mathbf{k}''' - (1/2)\mathbf{p}| > k_F} \frac{d\mathbf{k}''' \phi(|\mathbf{k}' - \mathbf{k}'''|) K(\mathbf{k}''', \mathbf{k}''; p, k_0)}{(k''')^2 - k_0^2} \tag{3.3}$$

where the p dependence of K comes from the Pauli principle and the k_0 dependence from the energy denominator. The ladder approximation to the ground-state energy per fermion is

$$\lim_{n \rightarrow \infty} \left[\frac{\Delta E_L M}{N \hbar^2} \right] = \frac{3}{8\pi k_F^3} \int d\mathbf{p} d\mathbf{k}_0 [vK(\mathbf{k}_0, \mathbf{k}_0; p, k_0) - K(\mathbf{k}_0, -\mathbf{k}_0; p, k_0)], \quad |\mathbf{k}_0 + \frac{1}{2}\mathbf{p}| \leq k_F; \quad |\mathbf{k}_0 - \frac{1}{2}\mathbf{p}| \leq k_F. \tag{3.4}$$

We have performed the computations by the methods of Brueckner and Masterson¹⁹ as implemented by Baker *et al.*²⁰ All the numerical approximations, parameters, etc. used are described in Refs. 15 and 20. We mention here only that v is chosen as 10^5 (instead of infinity) and c is the core radius. For the reader's convenience we also recall the formula

$$\rho = \frac{vk_F^3}{6\pi^2}, \tag{3.5}$$

which gives the Fermi momentum (the top of the Fermi sea in the noninteracting gas of point particles) in terms of the particle number per unit volume, ρ .

Our numerical results are given in Table I, and tabulated against the dimensionless density parameter $x = k_F c$. The errors due to the numerical solution of the K -matrix equation are believed to range from order 10^{-7} at $k_F c = 0.25$ to 10^{-3} at $k_F c = 1.50$. At $k_F c = 2$ we believe the accuracy to be a few tenths of a percent and a few percent at $k_F c = 3$. For the effect of total momentum averaging and the Pauli principle averaging the reader is referred to Baker, Ref. 15, and the references therein.

IV. PERTURBATION SERIES COEFFICIENTS

In order to carry out the L expansion in Sec. II, it is necessary to supply the expansion coefficients in (2.3) and

TABLE I. Ladder approximation to the ground-state energy shift of a hard sphere Fermi fluid.

x	$v=2$	$v=4$
0.00	0.0	0.0
0.25	$2.033\ 148 \times 10^{-3}$	$5.961\ 01 \times 10^{-3}$
0.50	$2.155\ 82 \times 10^{-2}$	$6.067\ 78 \times 10^{-2}$
0.75	$9.899\ 29 \times 10^{-2}$	0.268 483
1.00	0.322 295	0.849 344
1.25	0.865 559	2.234 35
1.50	2.050 79	5.217 71
2.00	9.028 99	22.5266
3.00	97.2263	234.997

(2.4) as a function of density. The first three orders are illustrated in Figs. 2 and 3. The corresponding equations are (see Baker, Ref. 15, Sec. IV C)

$$B_1 = \frac{3}{2^6 \pi^4} \int_{|\mathbf{m}| \leq 1, |\mathbf{n}| \leq 1} d\mathbf{m} d\mathbf{n} [v\phi(0) - \phi(|\mathbf{m} - \mathbf{n}|)], \tag{4.1}$$

which can be evaluated analytically for the potential (2.2) to give

$$B_1 = \frac{(k_F c)^3}{9\pi} \left\{ v - \frac{72}{y^6} [y^3 \text{Si}(y) - 4 - 3y^2 + (4 + y^2) \cos y + 4y \sin y] \right\}, \tag{4.2}$$

where $y = 2k_F c$, $\text{Si}(y)$ is the sine integral, and we use the result,

$$\phi(q) = 4\pi [\sin(qk_F c) - qk_F c \cos(qk_F c)] / q^3, \tag{4.3}$$

for the Fourier transform of the potential (2.2) with q the momentum in units of k_F .

The remaining expressions are

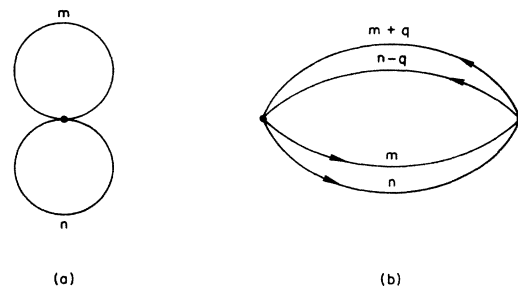


FIG. 2. The first, B_1 (a), and second, B_2 (b), order perturbation expansion terms. The line labels denote the momenta of the lines and refer to Eqs. (4.1) and (4.4).

$$B2 = \frac{-3\nu}{2^9 \pi^7 (k_{FC})^2} \int d\mathbf{m} d\mathbf{n} d\mathbf{q} \frac{\phi(q) \left[\phi(q) - \frac{1}{\nu} \phi(|\mathbf{n} - \mathbf{m} - \mathbf{q}|) \right]}{q^2 + \mathbf{q} \cdot (\mathbf{m} - \mathbf{n})}, \quad (4.4)$$

$$B3 = \frac{3\nu}{2^{12} \pi^{10} (k_{FC})^4} \int \frac{d\mathbf{m} d\mathbf{n} d\mathbf{q} d\mathbf{q}_1 \phi(q) \phi(|\mathbf{q} - \mathbf{q}_1|) \left[\phi(\mathbf{q}_1) - \frac{1}{\nu} \phi(|\mathbf{m} - \mathbf{n} + \mathbf{q}_1|) \right]}{[q^2 + \mathbf{q} \cdot (\mathbf{m} - \mathbf{n})][q_1^2 + \mathbf{q}_1 \cdot (\mathbf{m} - \mathbf{n})]}, \quad (4.5)$$

$$H3 = \frac{3\nu}{2^{12} \pi^{10} (k_{FC})^4} \int \frac{d\mathbf{m} d\mathbf{n} d\mathbf{q} d\mathbf{q}_1 \phi(q) \phi(\mathbf{q}_1) \left[\phi(|\mathbf{q} - \mathbf{q}_1|) - \frac{1}{\nu} \phi(|\mathbf{q} + \mathbf{q}_1 + \mathbf{m} - \mathbf{n}|) \right]}{[q^2 + \mathbf{q} \cdot (\mathbf{m} - \mathbf{n})][q^2 - q_1^2 + (\mathbf{q} - \mathbf{q}_1) \cdot (\mathbf{m} - \mathbf{n})]}, \quad (4.6)$$

$$R3 = \frac{3\nu^3}{2^{11} \pi^{10} (k_{FC})^4} \int d\mathbf{m} d\mathbf{n} d\mathbf{q} d\mathbf{q}_1 \left\{ \left[\phi(q) - \frac{1}{\nu} \phi(|\mathbf{m} + \mathbf{q} - \mathbf{q}_1|) \right] \left[\phi(q) - \frac{1}{\nu} \phi(|\mathbf{n} - \mathbf{q}_1|) \right] \right. \\ \times \left[\phi(q) - \frac{1}{\nu} \phi(|\mathbf{n} - \mathbf{m} - \mathbf{q}|) \right] - (\nu^{-1} - \nu^{-3}) \phi(|\mathbf{n} - \mathbf{m} - \mathbf{q}|) \\ \left. \times \phi(|\mathbf{m} + \mathbf{q} - \mathbf{q}_1|) \phi(|\mathbf{n} - \mathbf{q}_1|) \right\} / [q^2 + \mathbf{q} \cdot (\mathbf{m} - \mathbf{n})][q^2 + \mathbf{q} \cdot (\mathbf{m} - \mathbf{q}_1)], \quad (4.7)$$

$$F3 = \frac{-3\nu}{2^{11} \pi^{10} (k_{FC})^4} \int \frac{d\mathbf{m} d\mathbf{n} d\mathbf{q} d\mathbf{q}_1 \phi(q) \left[\phi(q) - \frac{1}{\nu} \phi(|\mathbf{n} - \mathbf{m} - \mathbf{q}|) \right]}{[q^2 + \mathbf{q} \cdot (\mathbf{m} - \mathbf{n})]^2} [\phi(|\mathbf{q} + \mathbf{m} + \mathbf{q}_1|) - \phi(|\mathbf{m} + \mathbf{q}_1|)], \quad (4.8)$$

where the region of integration includes all values of the momenta allowed by the Pauli exclusion principle. Thus, for example, all hole-line states are integrated over $|\mathbf{m}| \leq 1$ and all filled state momenta above the Fermi sea

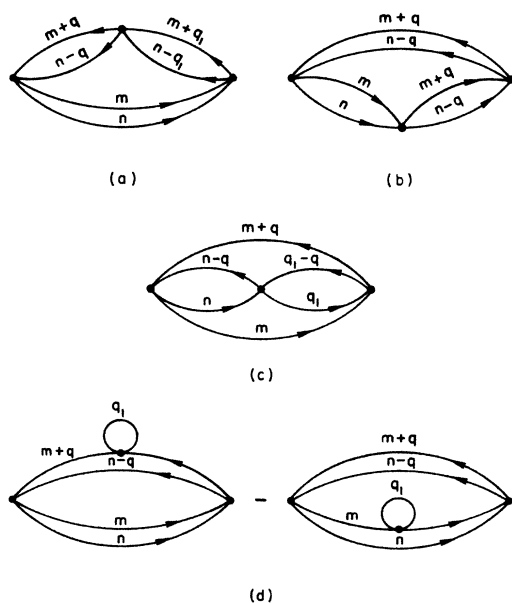


FIG. 3. The third-order perturbation expansion terms. (a) is the ladder graph $B3$, Eq. (4.5); (b) is the hole-hole scattering graph $H3$, Eq. (4.6); (c) is the ring diagram $R3$, Eq. (4.7); and (d) is the difference of diagrams with the first self-energy correction to a filled-state line and to a hole state line, $F3$, Eq. (4.8).

are integrated over $|\mathbf{m} + \mathbf{q}| > 1$. The line labels are given in Figs. 2 and 3.

We have performed these integrations by means of Monte Carlo evaluations. We select the momenta so that every point we choose makes a roughly equal contribution. For example, the independent momenta in the Fermi sea are chosen, as $m^3 = r_1$ with r_1 distributed uniformly on the unit interval 0 to 1. For a filled-state momentum which can be infinite we choose, say $|\mathbf{m} + \mathbf{q}| = r_2^{-E}$ where r_2 is distributed as was r_1 . The parameter E is chosen so the integrand (with respect to dr_2) goes to a constant as $r_2 \rightarrow 0$. Further details are given in Baker *et al.*²⁰ We have used 1×10^6 Monte Carlo repetitions for $B2$ and $B3$ and 5×10^5 for $H3$, $R3$, and $F3$.

Our results for $\nu=4$ are listed in Table II for the momenta $k_{FC}=0.25, 0.50, 0.75, 1.00, 1.25, 1.50, 2.00,$ and 3.00 , together with the observed standard deviations. We have gathered the corresponding results for $\nu=2$ together in Table III from Baker¹⁵ for the convenience of the reader. The column for $k_{FC}=1.25$, is new with this work. We remark in passing that in Baker (Ref. 15) the following two misprints were noted for $k_{FC}=1.5$: I-A.2 has the value -4.56×10^{-5} and II.8 has the value -6.32×10^{-6} instead of the values -4.56×10^{-4} and -6.23×10^{-5} given therein. The rows in Tables II and III marked $\Sigma 3, \Delta 3, \Sigma 4,$ and $\Delta 4$ are the complete sum third order, the sum of all third order diagrams except the ladder diagram $B3$, the complete sum fourth order, and the complete sum of all fourth order diagrams except the ladder diagram I.1, respectively.

Since all the diagrams except $R3$ are linear functions of ν we can, for general ν , compute

TABLE II. Monte Carlo calculations, $\nu=4$.

Diagram	$k_{Fc}=0.25$		$k_{Fc}=0.50$		$k_{Fc}=0.75$		$k_{Fc}=1.00$	
	Value	Deviation	Value	Deviation	Value	Deviation	Value	Deviation
B1	1.661993×10^{-3}		1.339353×10^{-2}		4.573553×10^{-2}		0.110973	
B2	-5.85×10^{-4}	3.7×10^{-6}	-4.01×10^{-3}	1.1×10^{-5}	-1.124×10^{-2}	2.1×10^{-5}	-2.163×10^{-2}	3.5×10^{-5}
B3	2.13×10^{-4}	2.2×10^{-6}	1.234×10^{-3}	4.8×10^{-6}	2.915×10^{-3}	8.6×10^{-6}	4.58×10^{-3}	1.4×10^{-4}
R3	2.20×10^{-6}	1.3×10^{-8}	4.82×10^{-5}	2.1×10^{-7}	2.49×10^{-4}	1.2×10^{-6}	7.34×10^{-4}	4.5×10^{-6}
H3	5.26×10^{-7}	6.4×10^{-9}	1.324×10^{-5}	5.6×10^{-8}	7.70×10^{-5}	3.7×10^{-7}	2.37×10^{-4}	1.1×10^{-6}
F3	1.17×10^{-7}	6.6×10^{-9}	6.23×10^{-6}	8.3×10^{-8}	5.63×10^{-5}	4.4×10^{-7}	2.32×10^{-4}	1.4×10^{-6}
$\Sigma 3$	2.16×10^{-4}	2.2×10^{-6}	1.302×10^{-3}	4.8×10^{-6}	3.297×10^{-3}	8.7×10^{-6}	5.79×10^{-3}	1.4×10^{-4}
$\Delta 3$	2.84×10^{-6}	1.6×10^{-8}	6.77×10^{-5}	2.3×10^{-7}	3.82×10^{-4}	1.3×10^{-6}	1.208×10^{-3}	4.8×10^{-6}

$$B2(\nu) = \frac{1}{2}[(\nu-2)B2(\nu=4) - (\nu-4)B2(\nu=2)], \quad (4.9)$$

for example. For R3 we have added the value for $\nu=1$ in Table IV. We obtain for general ν the extrapolation formula

$$\begin{aligned} R3(\nu) = & \frac{1}{3}(\nu-2)(\nu-4)R3(\nu=1) \\ & - \frac{1}{2}(\nu-1)(\nu-4)R3(\nu=2) \\ & + \frac{1}{6}(\nu-1)(\nu-2)R3(\nu=4). \end{aligned} \quad (4.10)$$

V. ANALYSIS OF THE L EXPANSION

In order to analyze the L expansion, we must first produce it. To this end we use the data in Tables II and III which directly give the expansion coefficients k_i and m_i of equations (2.3) and (2.4), respectively. Since B1 and B2 are the only diagrams in first and second order in ν , it follows directly that $k_1=m_1$ and $k_2=m_2$. Thus we may write (2.6) as

$$\frac{\Delta EMc^2}{N\hbar^2} = L + p_3 L^3 + p_4 L^4 + \dots, \quad (5.1)$$

since $p_1=1$ and $p_2=0$ identically. We list in Table V the coefficients p_3 and p_4 . The large relative errors for p_4 are caused by the cancellation of the component terms.

In order to display the results of these expansions we

note, as in our previous work,⁵ that we expect ΔE to diverge like $(k_F - k_{F,B})^{-2}$ as the Fermi momentum approaches some quantum, random, close-packing value. The Fermi momentum $k_{F,B}$ is associated with the Bernal density of a hard sphere system. This is not to say that the true equation of state may not exhibit some sort of order-disorder phase transition at smaller k_F than $k_{F,B}$ rendering $k_{F,B}$ a reflection of a spinodal point. However, our remark is meant to motivate looking at

$$\begin{aligned} Q(L) &= \left[\frac{LN(k_{Fc})^3 \hbar^2}{L_H \Delta EMc^2} \right]^{1/2} \\ &= q_0 \left[1 - \frac{1}{2} p_3 L^2 - \frac{1}{2} p_4 L^3 + O(L^4) \right] \end{aligned} \quad (5.2)$$

instead of (5.1) directly. Here L_H is (2.4) for the case of the hard sphere systems. The values of L_H are those listed in Table I and $q_0 = [(k_{Fc})^3 / L_H]^{1/2}$ which, for the convenience of the reader, we list in Table VI. The values for $k_{Fc}=0$ are obtained from the low density expansion¹⁵ and not from the solution of the K -matrix equation. $Q(L_H)$ is expected to tend to zero near $k_{F,B}$ more or less linearly.

The development of the ground-state energy of quantum fluids as an expansion in the attractive part of the potential about the hard-sphere fluid as the unperturbed basis system has been presented in a series of papers.¹⁻¹² Clearly a key step in this approach is an accurate re-

TABLE III. Monte Carlo calculations, $\nu=2$.

Diagram	$k_{Fc}=0.25$		$k_{Fc}=0.50$		$k_{Fc}=0.75$		$k_{Fc}=1.00$	
	Value	Deviation	Value	Deviation	Value	Deviation	Value	Deviation
B1	5.567499×10^{-4}		4.551588×10^{-3}		1.589397×10^{-2}		3.936174×10^{-2}	
B2	-1.960×10^{-4}	1.2×10^{-6}	-1.346×10^{-3}	2.4×10^{-6}	-3.827×10^{-3}	4.6×10^{-6}	-7.495×10^{-3}	1.9×10^{-5}
B3	7.003×10^{-5}	5.7×10^{-7}	4.146×10^{-4}	1.7×10^{-6}	9.742×10^{-4}	3.1×10^{-6}	1.538×10^{-3}	5.0×10^{-6}
R3	1.75×10^{-7}	1.6×10^{-9}	4.45×10^{-6}	4.3×10^{-8}	2.57×10^{-5}	2.0×10^{-7}	7.87×10^{-5}	5.6×10^{-7}
H3	-8.60×10^{-7}	6.8×10^{-9}	-2.14×10^{-5}	1.6×10^{-7}	-1.175×10^{-4}	6.4×10^{-7}	-3.30×10^{-4}	1.7×10^{-6}
F3	3.95×10^{-8}	2.3×10^{-10}	2.10×10^{-6}	5.0×10^{-8}	1.89×10^{-5}	2.5×10^{-7}	8.08×10^{-5}	8.3×10^{-7}
$\Sigma 3$	6.939×10^{-5}	5.7×10^{-7}	4.00×10^{-4}	1.7×10^{-6}	9.013×10^{-4}	3.2×10^{-6}	1.368×10^{-3}	5.3×10^{-6}
$\Delta 3$	-6.46×10^{-7}	7.0×10^{-9}	-1.48×10^{-5}	1.7×10^{-7}	-7.28×10^{-5}	7.2×10^{-7}	-1.70×10^{-4}	2.0×10^{-6}
I.1	-2.506×10^{-5}	1.9×10^{-7}	-1.288×10^{-4}	4.4×10^{-7}	-2.571×10^{-4}	1.1×10^{-6}	-3.347×10^{-4}	2.1×10^{-6}
$\Sigma 4$	-2.438×10^{-5}	1.9×10^{-7}	-1.152×10^{-4}	5.5×10^{-7}	-2.000×10^{-4}	1.4×10^{-6}	-2.24×10^{-4}	2.9×10^{-6}
$\Delta 4$	6.75×10^{-7}	7.0×10^{-9}	1.359×10^{-5}	3.3×10^{-7}	5.71×10^{-5}	8.7×10^{-7}	1.105×10^{-4}	2.0×10^{-6}

TABLE II. (Continued).

$k_{FC}=1.25$		$k_{FC}=1.50$		$k_{FC}=2.00$		$k_{FC}=3.00$	
Value	Deviation	Value	Deviation	Value	Deviation	Value	Deviation
0.2190174		0.3862495		0.9559854		3.484560	
-3.373×10^{-2}	5.4×10^{-5}	-4.606×10^{-2}	7.8×10^{-5}	-6.88×10^{-2}	1.5×10^{-4}	-0.1069	3.5×10^{-4}
5.67×10^{-3}	2.0×10^{-5}	6.06×10^{-3}	2.6×10^{-5}	5.76×10^{-3}	4.3×10^{-5}	5.247×10^{-2}	9.6×10^{-5}
1.68×10^{-3}	1.2×10^{-5}	3.35×10^{-3}	2.8×10^{-5}	1.009×10^{-2}	9.8×10^{-5}	3.40×10^{-2}	5.1×10^{-4}
5.04×10^{-4}	2.3×10^{-6}	8.42×10^{-4}	4.0×10^{-6}	1.459×10^{-3}	9.5×10^{-6}	1.92×10^{-3}	3.0×10^{-5}
6.55×10^{-4}	3.5×10^{-5}	1.377×10^{-3}	7.0×10^{-6}	3.69×10^{-3}	2.0×10^{-6}	8.98×10^{-3}	8.2×10^{-5}
8.51×10^{-3}	4.2×10^{-5}	1.163×10^{-2}	3.9×10^{-5}	2.100×10^{-2}	1.1×10^{-4}	9.74×10^{-2}	5.3×10^{-4}
2.84×10^{-3}	3.7×10^{-5}	5.57×10^{-3}	2.9×10^{-5}	1.524×10^{-2}	9.8×10^{-5}	4.49×10^{-2}	5.2×10^{-4}

sensation of the hard-sphere fluid ground-state energy. That approach was to sum judiciously the known appropriate low-density expansions to estimate this energy. For $\nu=2$, the energy is known to order $(k_{FC})^6$ and for

$\nu=4$ to order $(k_{FC})^6 \ln k_{FC}$. Such logarithmic terms do not appear at this order for $\nu=2$ because of the Pauli principle. In Ref. 5 the following results were presented: For $\nu=2$ the total energy is given by

$$\frac{EMc^2}{N\hbar^2} \cong \frac{3}{10} (k_{FC})^2 \left[\frac{1 + 0.699968(k_{FC})}{1 + 0.523153(k_{FC}) - 0.169644(k_{FC})^2 - 0.188781(k_{FC})^3} \right]^2, \quad (5.3)$$

which has a second order pole at $k_{FC}=1.939$, the predicted quantum random close packing or Bernal density for this system. This form was obtained by forming Padé approximants²¹ to the square root of the reciprocal of $\epsilon_0(k_{FC})=10EM/(3N\hbar^2 k_F^2)$ in order to ensure a second order pole in E as suggested by the uncertainty principle.

For $\nu=4$, a generalized version of the Padé approximant is used to accommodate the logarithmic term. The representation

$$\frac{EMc^2}{N\hbar^2} \cong \frac{3}{10} (k_{FC})^2 \left[\frac{1 + 4.03606(k_{FC})}{1 + 3.50554(k_{FC}) - 1.99733(k_{FC})^2 - 0.704299(k_{FC})^4 \ln(k_{FC})} \right]^2 \quad (5.4)$$

was adopted in Ref. 5, which again has a positive, real, second-order pole as does (5.3). It is placed at $\rho_B/\rho_0=0.173$ where $\rho_0=\sqrt{2}/c^3$ is the regular, classical, close packed face-centered-cubic density. This value is very close to $\rho_B/\rho_0=0.174$ found from (5.3) for the $\nu=2$ case, and is less than $\rho_B/\rho_0=0.355$ found¹ for a hard-sphere Bose fluid which in turn is less than the empirical classical value²² of $\rho_B/\rho_0=0.86$.

The representation (5.4) agrees, as it should, with the low density expansion for $\nu=4$

$$\begin{aligned} \frac{EMc^2}{N\hbar^2} = \frac{3}{10} (k_{FC})^2 [& 1 + 1.061033(k_{FC}) + 0.556610(k_{FC})^2 \\ & + 1.300620(k_{FC})^3 \\ & - 1.408598(k_{FC})^4 \ln(k_{FC}) + \dots] \end{aligned} \quad (5.5)$$

through the order $(k_{FC})^6 \ln(k_{FC})$. It is not unique but was selected as detailed in Ref. 5.

TABLE III. (Continued).

$k_{FC}=1.25$		$k_{FC}=1.50$		$k_{FC}=2.00$		$k_{FC}=3.00$	
Value	Deviation	Value	Deviation	Value	Deviation	Value	Deviation
8.086206×10^{-2}		1.475170×10^{-1}		3.901006×10^{-1}		1.574696	
-1.200×10^{-2}	2.2×10^{-5}	-1.715×10^{-2}	4.8×10^{-5}	-2.868×10^{-2}	5.9×10^{-3}	-5.367×10^{-2}	3.4×10^{-4}
1.968×10^{-3}	7.9×10^{-6}	2.190×10^{-3}	1.1×10^{-5}	2.44×10^{-3}	2.0×10^{-3}	2.73×10^{-3}	1.2×10^{-4}
-6.11×10^{-4}	2.3×10^{-6}	2.81×10^{-4}	2.2×10^{-6}	4.99×10^{-4}	5.7×10^{-6}	8.21×10^{-4}	2.1×10^{-5}
1.686×10^{-4}	7.8×10^{-7}	-7.98×10^{-4}	7.7×10^{-6}	-2.61×10^{-4}	1.3×10^{-5}	4.75×10^{-3}	2.0×10^{-4}
2.32×10^{-4}	1.3×10^{-6}	5.05×10^{-4}	4.6×10^{-6}	1.51×10^{-3}	1.5×10^{-5}	4.45×10^{-3}	6.6×10^{-5}
1.758×10^{-3}	8.4×10^{-6}	2.178×10^{-3}	1.4×10^{-5}	4.19×10^{-3}	2.9×10^{-5}	1.275×10^{-2}	2.4×10^{-4}
-2.10×10^{-4}	2.8×10^{-6}	-1.2×10^{-5}	9.2×10^{-6}	1.51×10^{-3}	2.1×10^{-5}	1.002×10^{-2}	2.1×10^{-4}
		-3.01×10^{-4}	4.7×10^{-6}	-2.25×10^{-4}	9.4×10^{-6}	-1.09×10^{-4}	2.8×10^{-5}
		-3.20×10^{-4}	8.2×10^{-6}	-1.111×10^{-3}	2.8×10^{-5}	-5.83×10^{-3}	2.6×10^{-4}
		-1.8×10^{-5}	6.7×10^{-6}	-8.86×10^{-4}	2.6×10^{-5}	-5.72×10^{-3}	2.6×10^{-4}

TABLE IV. Monte Carlo calculations, $\nu=1$.

k_{Fc}	R_3	Deviation
0.25	-8.2×10^{-11}	4.1×10^{-11}
0.50	-1.7×10^{-8}	1.8×10^{-9}
0.75	-3.8×10^{-7}	1.4×10^{-8}
1.00	-3.48×10^{-6}	6.9×10^{-8}
1.25	-1.79×10^{-5}	2.4×10^{-7}
1.50	-6.23×10^{-5}	6.5×10^{-7}
2.00	-3.34×10^{-4}	3.5×10^{-6}
3.00	-8.9×10^{-4}	3.2×10^{-5}
3.00	-8.8×10^{-4}	3.2×10^{-5}

TABLE V. L -expansion coefficients.

k_{Fc}	$\nu=4$		$\nu=2$	
	p_3	p_3	p_3	p_4
0.25	$6.19 \times 10^2 \pm 3.5$	$-3.74 \times 10^3 \pm 4.1 \times 10^1$	$-7.2 \times 10^4 \pm 1.1 \times 10^5$	
0.50	$2.818 \times 10^1 \pm 9.6 \times 10^{-2}$	$-1.57 \times 10^2 \pm 1.8$	$9.7 \times 10^2 \pm 8.5 \times 10^2$	
0.75	$3.99 \pm 1.4 \times 10^{-2}$	$-1.82 \times 10^1 \pm 1.8 \times 10^{-1}$	$6.9 \times 10^1 \pm 1.6 \times 10^1$	
1.00	$9.05 \times 10^{-1} \pm 3.6 \times 10^{-3}$	$-2.80 \pm 3.3 \times 10^{-2}$	$5.5 \pm 9.6 \times 10^{-1}$	
1.25	$2.70 \times 10^{-1} \pm 3.5 \times 10^{-3}$	$-3.97 \times 10^{-1} \pm 5.3 \times 10^{-3}$		
1.50	$1.43 \times 10^{-1} \pm 2.8 \times 10^{-3}$	$-3.7 \times 10^{-3} \pm 2.9 \times 10^{-3}$	$-4.8 \times 10^{-2} \pm 1.6 \times 10^{-2}$	
2.00	$1.74 \times 10^{-2} \pm 1.1 \times 10^{-4}$	$2.95 \times 10^{-2} \pm 3.5 \times 10^{-4}$	$-2.2 \times 10^{-2} \pm 1.1 \times 10^{-3}$	
3.00	$1.06 \times 10^{-3} \pm 1.2 \times 10^{-5}$	$2.57 \times 10^{-3} \pm 5.4 \times 10^{-5}$	$-7.6 \times 10^{-4} \pm 4.2 \times 10^{-5}$	

TABLE VI. Values of the initial coefficient q_0 in Eq. (5.2).

k_{Fc}	$\nu=2$	$\nu=4$
0.00	3.069 98	1.772 45
0.25	2.772 21	1.619 01
0.50	2.407 96	1.435 29
0.75	2.064 38	1.253 53
1.00	1.761 46	1.085 07
1.25	1.311 63	0.934 95
1.50	1.282 85	0.804 26
2.00	0.941 29	0.595 93
3.00	0.526 97	0.338 96

TABLE VII. $Q(L_H)$ for $\nu=2$.

k_{Fc}	L expansion	Eq. (5.3)	[1/3]
0.00	3.069 98	3.069 98	3.069 98
0.25	$2.794 \pm 6 \times 10^{-3}$	2.802 91	2.804 42
0.50	$2.49 \pm 1 \times 10^{-2}$	2.461 77	2.479 65
0.75	$2.19 \pm 2 \times 10^{-2}$	2.095 33	2.161 97
1.00	$1.86 \pm 5 \times 10^{-2}$	1.717 29	1.876 36
1.25	$1.5 \pm 2 \times 10^{-1}$	1.323 70	1.627 80
1.50	$1.3 \pm 2 \times 10^{-1}$	0.900 64	1.414 29

TABLE VIII. $Q(L_H)$ for $\nu=4$.

k_{Fc}	L expansion	Eq. (5.4)	Eq. (5.5)
0.00	1.77245	1.772 45	1.772 45
0.25	$1.601 \pm 3 \times 10^{-3}$	1.639 88	1.593 95
0.50	$1.36 \pm 3 \times 10^{-2}$	1.494 58	1.365 94
0.75	$1.08 \pm 1.5 \times 10^{-1}$	1.310 46	1.183 19
1.00	0.5 ± 0.5	1.048 62	1.068 75
1.25	*	0.666 92	1.024 61

We have summed directly the values of the series (5.2). In addition, we have used the method of Padé approximants²¹ to sum this series. Since the series (5.2), as well as (2.6), is most likely an asymptotic one, as a further refinement, we have also tried the Padé-Borel method²¹ which is adapted to this type of series. We found the Padé-Borel method to be no more efficient than the standard Padé method, probably because our series is rather short.

We summarize our conclusions for $\nu=2$ in Table VII.

From a review of the results of Table VII we see that the L expansion is quite accurate for small values of k_{FC} and deteriorates as k_{FC} increases. If we choose $c=0.4$ F and M to be the nucleon mass, then the error in the ground-state energy given by the L expansion would be about ± 0.04 MeV at $k_{FC}=0.50$, about ± 0.4 MeV at $k_{FC}=0.75$, and about ± 4 MeV at $k_{FC}=1.00$. Since $k_{FC}\simeq 0.69$ for neutron matter at the same density as nuclear matter, this accuracy should be sufficient to deal with that problem. The accuracy of the L expansion appears to us to be sufficient to reliably compute the ground-state energy of hard-sphere fluid systems which are quite dilute compared to the Bernal density. In the neutron matter problem, compared with the estimate of the Bernal density quoted above, the density is less than five percent of the Bernal density.

Some further conclusions can be drawn from Table VII. The $[1/3]$ Padé representation⁵ to $\epsilon^{-1/2}$ instead of the $[3/1]$ representation used in (5.3) gives a much better representation over the whole range of values given in that table and is our best summary of the low density data for the $\nu=2$ hard-sphere fermion fluid. This representation does not, however, predict a random close-packing density. For a truly accurate representation of systems with

higher density, such as liquid ^3H , more information from other methods, e.g., the quantum Green's function Monte Carlo (GFMC), will be required. Failing this information, we conclude that the $[1/3]$ approximant is the best summary currently available. The addition of high-density GFMC data was quite successful for hard-sphere boson fluids.^{1,2,5}

We summarize our conclusions for $\nu=4$ in Table VIII.

From a review of the results of Table VIII we see that the L expansion is quite accurate for small values of k_{FC} . It has an error which increases to around 1 MeV for $k_{FC}\simeq 0.50$. Since $k_{FC}\simeq 0.54$ for nuclear matter, this accuracy should be just sufficient for that rather dilute problem.

Some further conclusions are possible from the results reported in Table VIII. The truncated series Eq. (5.5) gives a much better representation in the low-density region than does that of (5.4), and is our best summary for the low-density ($k_{FC} < 0.6$) region. Unfortunately this representation does not predict a random close-packing density and, in fact, is thermodynamically unstable for $k_{FC} \geq 1.27$. As is evident from Table VIII, in order to carry these results to higher densities, exact high-density results, such as presumably could be obtained by GFMC methods, for example, are required. In the absence of further such information, we conclude that (5.5) is the best available summary of the low-density energy of the $\nu=4$ hard-sphere fermion fluid.

This work was supported in part by the U. S. Department of Energy. The work of G.B. and L.B. was also supported in part by NSF Grant INT-84-01865.

*Permanent address: Department of Physics, St. Louis University, St. Louis, MO 63103.

† Present address: Physics Department, North Dakota State University, Fargo, ND 58105.

¹G. A. Baker, Jr., M. de Llano, and J. Pineda, Phys. Rev. B **24**, 6304 (1981).

²G. A. Baker, Jr., M. de Llano, J. Pineda, and W. C. Stwalley, Phys. Rev. B **25**, 481 (1982).

³G. A. Baker, Jr., L. P. Benofy, M. Fortes, M. de Llano, S. M. Peltier, and A. Plastino, Phys. Rev. A **26**, 3575 (1982).

⁴G. A. Baker, Jr., M. de Llano, M. Fortes, L. P. Benofy, S. Peltier, and A. Plastino, Notas Fis. **5**, 47 (1982).

⁵G. A. Baker, Jr., G. Gutiérrez, and M. de Llano, Ann. Phys. (N.Y.) **153**, 283 (1984).

⁶G. A. Baker, Jr., M. Fortes, and M. de Llano, in *Recent Progress in Many-Body Theories*, edited by H. Kümmel and M. L. Ristig (Springer-Verlag, Berlin, 1984), p. 351.

⁷E. Buendía, R. Guardiola, and M. de Llano, Phys. Rev. A **30**, 941 (1984).

⁸G. A. Baker, Jr., An. Fis. **81**, 65 (1985).

⁹L. P. Benofy, An. Fis. **81**, 67 (1985).

¹⁰E. Buendía and R. Guardiola, An. Fis. **81**, 70 (1985).

¹¹G. Gutiérrez, M. de Llano, and W. C. Stwalley, Phys. Rev. B **29**, 5211 (1984).

¹²V. C. Aguilera-Navarro, G. A. Baker, Jr., L. P. Benofy, M. Fortes, and M. de Llano, submitted.

¹³J. A. Barker and D. Henderson, Rev. Mod. Phys. **48**, 587 (1976).

¹⁴K. A. Brueckner, Phys. Rev. **100**, 36 (1955).

¹⁵G. A. Baker, Jr., Rev. Mod. Phys. **43**, 479 (1971).

¹⁶G. A. Baker, Jr. and J. Kahane, J. Math. Phys. **10**, 1647 (1969).

¹⁷G. A. Baker, Jr., M. F. Hind, and J. Kahane, Phys. Rev. C **2**, 841 (1970).

¹⁸G. A. Baker, Jr. and H. J. Pirner, Ann. Phys. (N.Y.) **148**, 168 (1983).

¹⁹K. A. Brueckner and K. S. Masterson, Phys. Rev. **128**, 2267 (1962).

²⁰G. A. Baker, Jr., J. L. Gammel, and B. J. Hill, Phys. Rev. **132**, 1373 (1963).

²¹G. A. Baker, Jr. *Essentials of Padé Approximants* (Academic, New York, 1975); G. A. Baker, Jr. and P. R. Graves-Morris, in *Encyclopedia of Mathematics and its Applications*, edited by G.-C. Rota (Addison-Wesley, Reading, MA, 1981), Vols. 13 and 14.

²²J. D. Bernal and J. Mason, Nature (London) **188**, 910 (1960); J. D. Bernal, Proc. R. Soc. London Ser. A **280**, 299 (1964); G. D. Scott and D. M. Kilgour, J. Phys. D **2**, 863 (1969).